Shading Models for Illumination and Reflectance Invariant Shape Detectors

Peter Nillius†, Josephine Sullivan† and Antonis Argyros‡
KTH, Sweden†   FORTH, Greece‡

Overview

We present a method to construct robust shape detectors based on shading. The detectors consist of a PCA appearance model which is analytically computed from the image formation model.

Contributions:

- Extension of analytical/model-based PCA to include shape variations
- Shape detection proof of concept through the construction and evaluation of a sphere and a cylinder detector.

Shading in Frequency Space

We model shading from surfaces with any isotropic BRDF under any illumination. Using frequency space representations, this shading can be expressed as a linear combination of basis functions.

$$I_i = \sum_{k=1}^{N} c_k E_k(\alpha_i, \beta_i),$$

where

$$c_k = L_l^m b_{op}^q$$

- L_l^m - Light field coefficients
- b_{op}^q - BRDF coefficients
- $E_k(\alpha_i, \beta_i)$ - Reflectance map basis functions

We use $N = 2000$ number of basis functions to be able to represent shading from specular surfaces.

Model-Based PCA of Shading

The frequency space representation can be used to analytically derive the principal components of the set of images of a shape. The variations in the images are defined by the variations in the illumination and BRDF [4, 2, 3].

New Extension to Include Shape Variations

The principal components are the eigenvectors of the image covariance matrix, Σ_I. Using the frequency space representation this matrix can be computed as

$$\boldsymbol{\Sigma}_I = \sum_{s \in S} \mathbf{F}_s \mathbf{V}_c \mathbf{F}_s^T p_s(s)$$

where

- $\mathbf{V}_c$ - Light field and BRDF covariances
- $\mathbf{F}_s$ - Centered basis functions for shape s
- $p_s(s)$ - Probability prior for shape s

Eigenfaces from four 3D Meshes

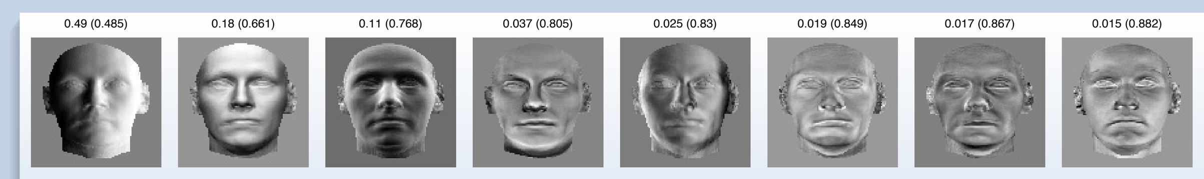

Human Skin BRDF

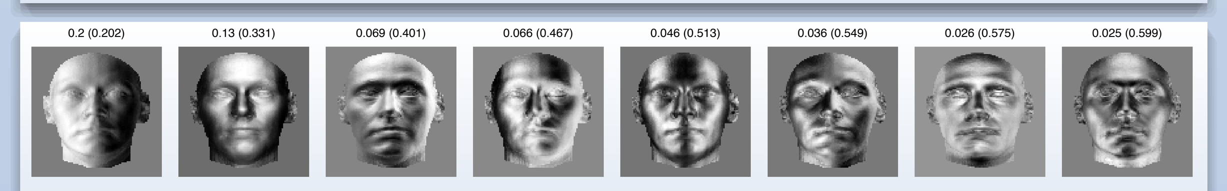

Torrance-Sparrow BRDF Mix

Shape Detection

Overall approach:

- Score based on normalized residual variance
- Run on scale-pyramid to cope with large scale variations
- Use multiple models to cope with large pose changes
- Train each model to cope with
  - small scale and pose changes
  - illumination changes
  - BRDF changes

Sphere and Cylinder Detectors

To evaluate the method we have created detectors for two shape primitives, spheres and cylinders.

Training for Pose Variations

The models were trained for micro-scale variations and sub-pixel translations. The eight cylinder models were additionally trained for micro-rotations.

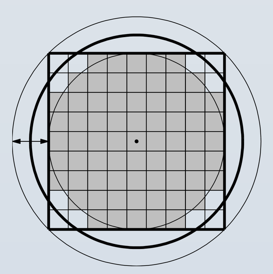

Micro-Scale Variations

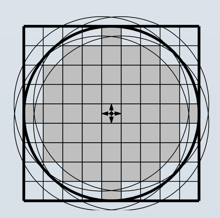

Sup-Pixel Translations

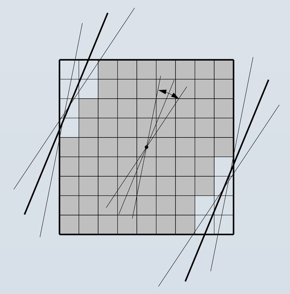

Micro-Rotations

Training for Lighting Variations

The lighting variations were modeled with nine HDR illumination maps each undergoing all 3D rotations.

Training for BRDF Variations

The BRDF variation were modeled with Torrance-Sparrow of varying specularity and surface roughness.

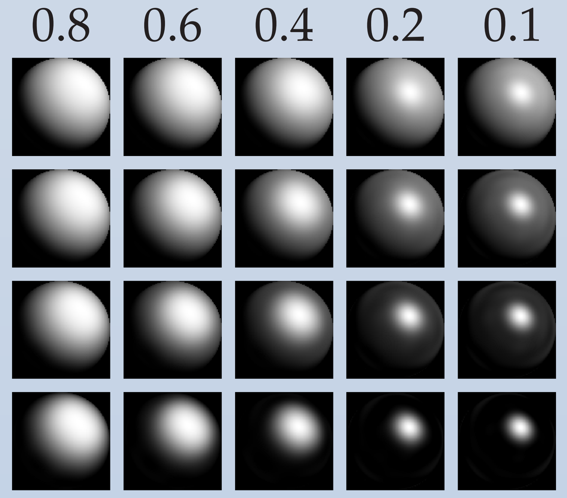

The Resulting Models

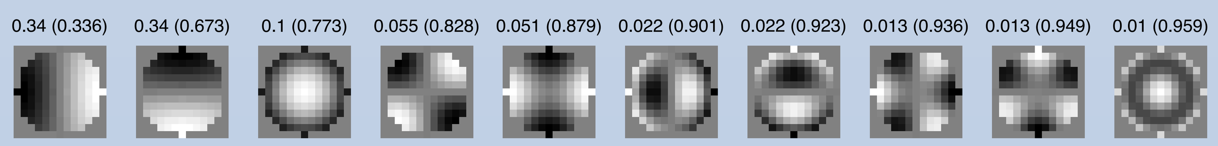

Sphere Basis Images

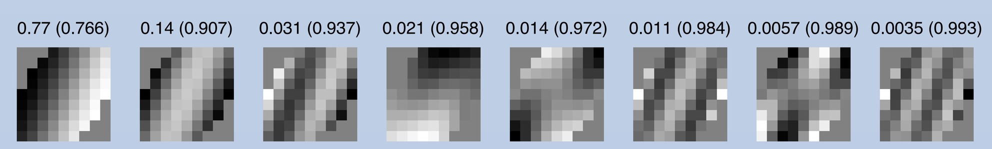

Cylinder Basis Images (one of eight directions)

Experiments

Synthetic experiments

The detectors have been tested on all combinations of lighting, BRDF and pose variations. Over 500 millions image patches have been used.

For each image patch the appearance basis is fitted and the variance of the residual is computed.

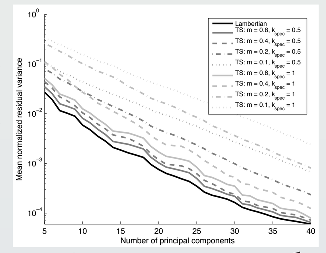

The BSDS300 data set [1] is used as negative exemplars when computing ROC-curves. To summarize these results we plot the equal error rates.

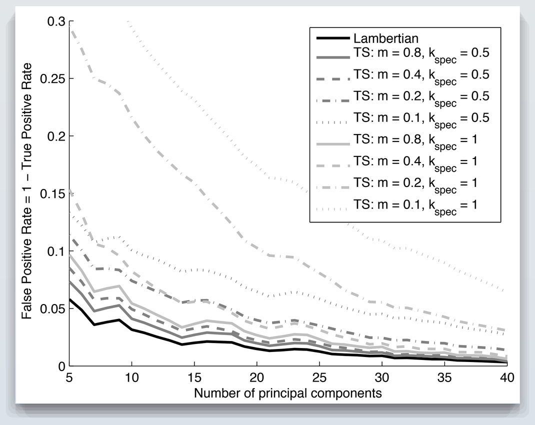

Sphere Detector

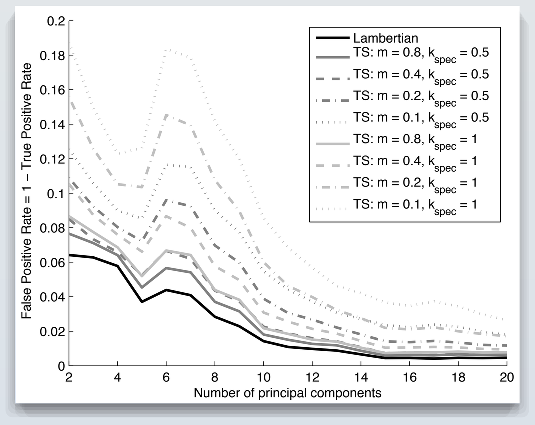

Cylinder Detector

The bases increasingly fit the shapes better than the negative exemplars with an increasing number of components.

Experiments on real images

We have created a dataset of 31 images containing three spheres, one paper, one silver painted and one gold painted which is more specular. The spheres are photographed in a number of different lighting conditions and scales.

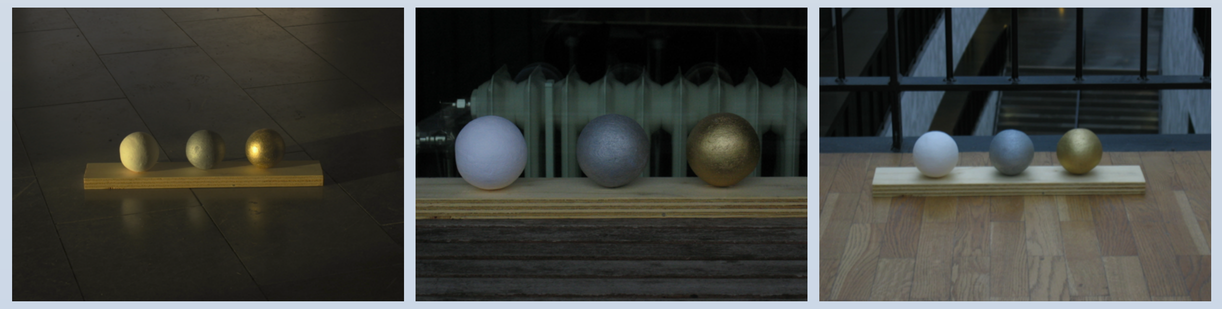

In comparison with BSDS300 the spheres fit the model better. More components leads to better discrimination.

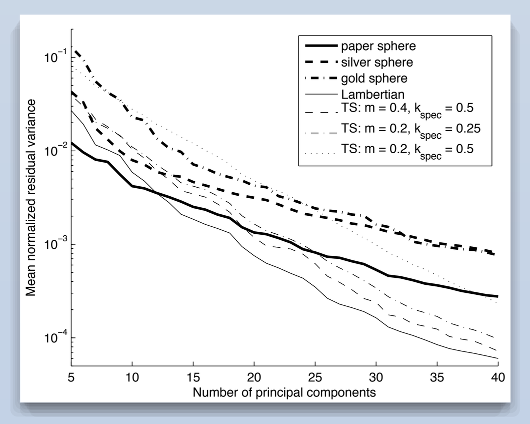

Residual Variance

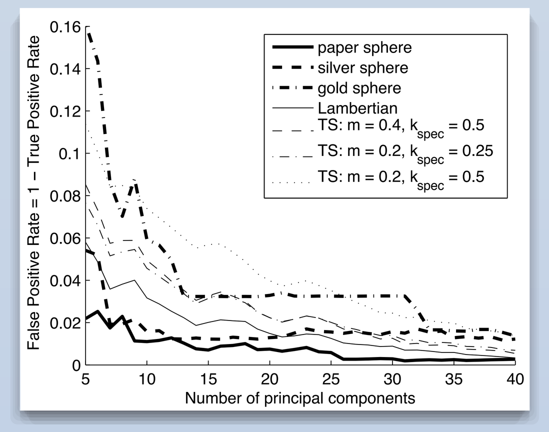

Equal Error

Examples

Sphere Detector

Best Score

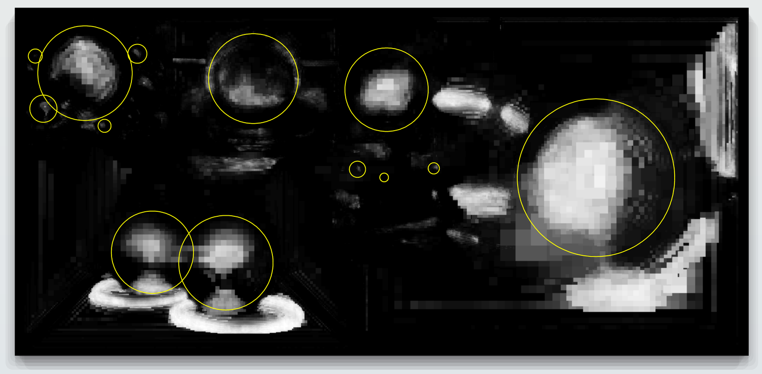

Best Scale

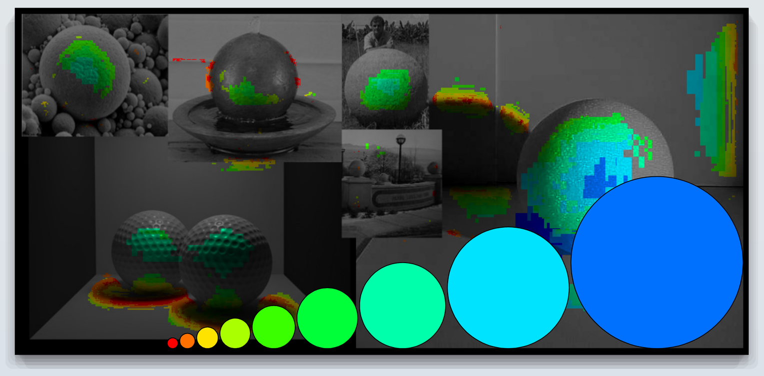

Cylinder Detector

Best Score

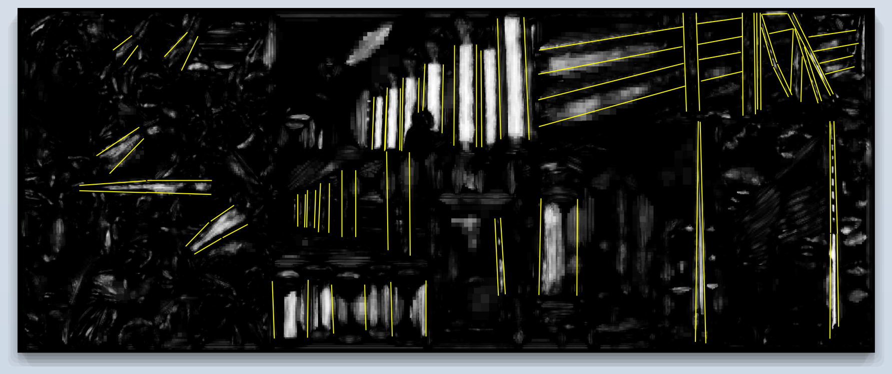

Best Scale

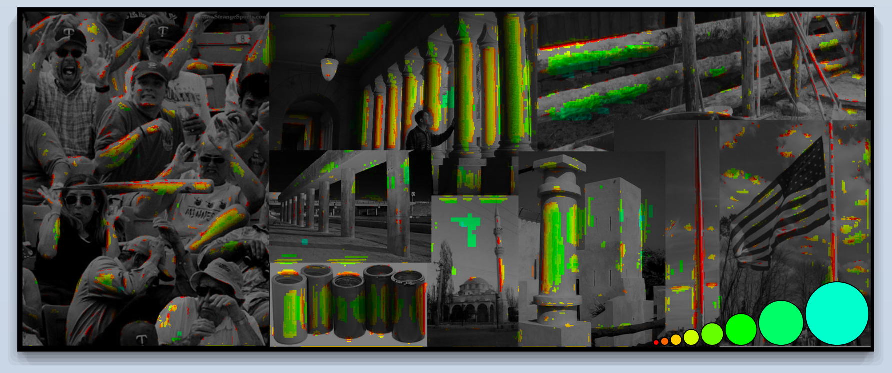

Best Direction

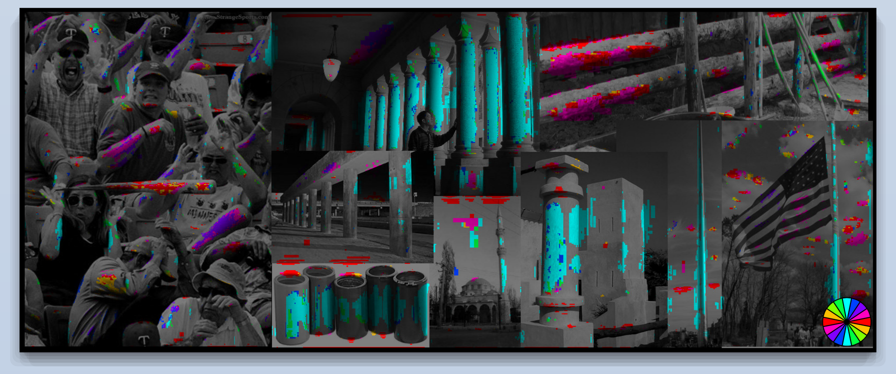

References

[1] D. Martin, C. Fowlkes, D. Tal, and J. Malik. A database of human segmented natural images and its appl. to evaluating segmentation algorithms and measuring ecological statistics. In *ICCV*, volume 2, pages 416–423, July 2007.

[2] P. Nillius and J. Eklundh. Low-dimensional representations of shaded surfaces under varying illumination. In *CVPR*, pages II:185–192, 2003.

[3] P. Nillius and J. Eklundh. Phenomenological eigenfunctions for image irradiance. In *ICCV*, pages 568–575, 2003.

[4] R. Ramamoorthi. Analytic pca construction for theoretical analysis of lighting variability in images of a lambertian object. *IEEE PAMI*, 24(10):1322–1333, October 2002.